Spectroscopic study of tetradecyltrimethylammonium bromide Pt-C_{14}TAB nanoparticles: Structure and Stability

Yuri Borodko,[a] Louis Jones,[b] Hyunjoo Lee,[b] Heinz Frei[c] and Gabor Somorjai[a,b]*

a) Chemical and Materials Sciences Divisions, Lawrence Berkeley National Laboratory, 1 Cyclotron Road, Berkeley CA 94720
b) Department of Chemistry, University of California, Berkeley, CA 94720
c) Physical Biosciences Division, Lawrence Berkeley National Laboratory

Abstract

The vibrational spectra of platinum nanoparticles (12 nm) capped with tetradecyltrimethylammonium bromide, C_{14}TAB, were investigated by Fourier transform infrared (FTIR) spectroscopy. We have shown that the thermal decay of Pt-C_{14}TAB nanoparticles in N_2, H_2 and O_2 atmospheres leads to the release of hydrocarbon chain of surfactant and the formation of strongly bonded layer of ammonium cations on the platinum surface. The platinum atoms accessible to CO chemisorptions were not reducible by hydrogen in the temperature ranging from 30°C to 200°C. A FTIR spectrum of C_{14}TAB adsorbed on Pt nanoparticles dramatically perturbed as compared with pure C_{14}TAB. New intense and broad bands centered at 1450 cm^{-1} and 760 cm^{-1} are making their appearance in Pt-C_{14}TAB. It may be speculated, that new bands are result of coupling between conducting electrons of Pt and molecular vibrations of adsorbed C_{14}TAB and as a consequence specific vibrational modes of ammonium cation transformed into electron-vibrational modes.

Introduction

Metallic nanoparticles with narrow size distributions and distinct morphologies make them very intriguing candidates for the development of novel highly selective catalysts [1]. The knowledge of the structure and properties of the interface between the capping agent and the metal surface is critical when incorporating metallic nanoparticles into catalytic reactions, since capping agents as ligands can stabilize specific electronic states of the surface atoms, thus creating catalytic active sites. A routine procedure to activate heterogeneous catalysts is Redox cycling treatment of the catalysts at elevated temperatures. This may induce changes in the electronic structure of metallic atoms, the size and shape of the nanoparticles, the chemical state of the capping agent, and the size of metallic surface that is accessible to reactant. Cetyltrimetilammonium bromide (C_{15}TAB) has been used as a surface stabilizer of metallic nanocrystals with different shapes and sizes [2]. Several studies concerning the adsorption of CTAB on solid surfaces were performed [3]. El-Sayed and Nikoobakht showed evidence for bilayer assembly of cationic surfactants on the surface of gold nanorods. They showed that heating of Au-CTAB nanoparticles in air up to 350 °C desorbed methylene tails while large amounts of ammonium cation heads remained present on the gold surface [4]. Tetradecyltrimethylammonium bromide or C_{14}TAB is an ionic, amphiphilic surfactant, and the electrostatic interactions with the metallic surface play a dominant role in stabilizing nanoparticles. The tetrahedral cation N^+ is isoelectronic and structurally equivalent to carbon in the sp^3 state and is unable to participate in donor-acceptor interactions. This makes it different from another popular capping agent of metallic nanoparticles, poly(vinylpyrrolidone) (PVP), which has electron-donating groups -

pyrrolidone rings - making charge-transfer interactions the dominant factor in stabilizing the nanoparticles [5]. Several experimental techniques have been used to explore the interfaces of Ag-CTAB [2] and Au-CTAB [4] including FTIR, Raman, TEM, TGA, and UV-VIS.

In this paper, we report a study of the structure and stability of C_{14}TAB-capped Pt nanocrystals using primarily in-situ vibrational spectroscopy measurements. We present results of the thermal decay of C_{14}TAB bonded to Pt nanocrystals in N_2, H_2/Ar, and O_2 atmospheres. We have concluded that the thermal decay of bonded C_{14}TAB results in platinum particles being stabilized by only the ammonium-'head' while the hydrocarbon 'tail' evolves into the gas phase. It was found that after heating in hydrogen above 200 °C, the active surface area of the platinum nanoparticles becomes inaccessible for carbon monoxide due to the formation of a shield of ammonium cations. This result differs from the mechanism of thermal degradation of pure C_{14}TAB under the same conditions in which unimolecular decay of CTAB leads to the release of both the hydrocarbon 'tail' and the ammonium 'head' into the gas phase. The Pt-C_{14}TAB FTIR spectra show the appearance of unusually high-intensity and broad bands centered at 760 and 1450 cm^{-1}. We attribute this phenomenon to the existence of electron-molecular vibration *(e - mv)* coupling between conducting electrons of Pt nanoparticles and intramolecular vibrations of adsorbed ammonium cations.

Experimental Section

Synthesis and Assembly of Platinum Nanoparticles. Nanoparticles stabilized with tetradecyltrimethylammonium bromide (TTAB) were prepared by mixing aqueous solutions of K_2PtCl_4 (99.9% pure from Alfa Aesar) and TTAB (99% pure from Aldrich)

in a 20mL vial at room temperature [1]. The concentration of K_2PtCl_4 and $C_{14}TAB$ in the reactant solution was 1.5mM and 150mM, respectively. The mixture was heated at 323K for ~5min until the solution became clear. After the addition of ice-cold $NaBH_4$ (99% pure from Aldrich), the vial was capped with a rubber septum and the H_2 gas was flowed for 5min and pressurized for 1min. The concentration of $NaBH_4$ was 5mM. After the removal of the needle, the solution was kept at 323K for 6h. The nanoparticles were centrifuged at 3krpm for 30min. The precipitates were discarded and the supernatant solution was centrifuged again at 14krpm for 10min. The supernatant was discarded and the precipitates were re-dispersed in DI water with sonication. The solution was centrifuged at 14krpm for 10min once more, and the precipitates were collected and re-dispersed in DI water. These washed nanoparticles were used for spectroscopic and TEM measurement (FEI Tecnai 12 TEM, measured at 100kV) and further assembly (Figure 1A). The average size of Pt nanoparticles was 12 ± 2nm (vertex-to-vertex).

Nanoparticles were assembled and deposited on silicon or germanium substrates by the Langmuir-Blodgett (LB) technique. Colloidal Pt solutions were dispersed on the surface of deionized water (18 MΩ·cm) on a LB trough (NIMA, type 611) at room temperature. The compact nanoparticle surface layer was prepared by compressing a mobile barrier at a rate of $20cm^2$/min. Then, the nanoparticles were deposited on the substrates by lifting up the substrates, which had been immersed in the water subphase before the nanoparticles were dispersed, at a surface pressure of ~15 mN/m. XPS technique was used to detect the presence of bromine on the surface of Pt-$C_{14}TAB$ nanoparticles. XPS spectra were taken on a 15 kV, 350 Watt PHI 5400 ESCA/XPS system equipped with an Al anode X-ray source. In order to minimize contamination of

the sample with free non-bonded C_{14}TAB, which was observed in drop-cast film, a Langmuir-Blodgett film of Pt-C_{14}TAB deposited on Si-wafer was analyzed (Figure 1B). It was found that ratio of intensities (normalized on factor for cross-section for photo ionization) for Br 3d at 69 eV; Br 3p at 182 eV lines and Pt $4f_{7/2}$ line at 74.8 eV is less than 0.05:1=Br: Pt [6]. Thermogravimetric analyses (TGA) were performed on a TA Instruments SDT 2960 Integrated TGA/DSC analyzer with a heating rate of 10 ºC min^{-1} under a flow of nitrogen.

Spectroscopic Characterisation.

DRIFT-FTIR spectra were measured on a Nicolet Nexus-670 spectrophotometer with integrated diffuse reflectance optics (Spectra-Tech Collector II). It was found that improved spectra could be obtained from a thin layer of M-PVP (M = Pt, Rh) prepared by evaporation of chloroform or ethanol solutions onto a reflective surface such as aluminum or gold foil. Since the layer thickness can be adjusted to render the sample partially IR transparent, we were able to optimize the ratio of diffuse-to-specular reflectance and obtain spectra of similar quality compared to those measured in transmission mode. A Temperature/Vacuum chamber Spectra-Tech 0030-101 was used for in situ FTIR measurements in N_2, H_2/Ar (10 % H_2) and O_2 flow.

UV-VIS spectra of C_{14}TAB and Pt-C_{14}TAB deposited on Al-foil were measured by Perkin-Elmer Lambda 650 spectrophotometer equipped with a 60 mm Spectralon integrating sphere.

The UV-Raman spectroscopy system was used to monitor the spectrum of Pt-C_{14}TAB. A continuous wave (cw) intracavity doubled argon ion laser operating at 244 nm was used as the excitation source. To prepare samples for Raman studies, solutions of Pt-

C_{14}TAB in water were evaporated onto 15-mm diameter Al foil substrates. The Raman System is described in detail elsewhere [5].

An oil-free Alcatel Drytel 34 turbopump station was used for sample evacuation. Grams/AI and Omnic software from Thermo Galactic were used for processing DRIFT and ATR-FTIR spectra.

RESULTS and DISCUSSION

.

Vibrational Spectra of C_{14}TAB. FTIR-DRIFT and Raman (UV-VIS) vibrational spectra of C_{14}TAB are shown in Figure 2a. In both FTIR and UV-Raman, the CH stretch modes give rise to the most intense bands. Analysis of infrared and Raman spectra of CTAB was considered recently [7]. The observed bands may be subdivided into two categories: bands related to the vibrations of the trimethylammonium head and to the vibrations of the alkane tail. We used the interpretation of infrared spectra of deuterated methylammonium cations given by Ebsworth and Sheppard [8] and the results of *ab initio* LCAO-MO-SCF and DFT calculations [7] to identify the spectroscopic signatures of the tetramethylammonium cation. The alkyl tail has some well-established IR-bands [9]. The experimental bands and assignments for FTIR and UV-Raman spectra of C_{14}TAB are presented in the first and third columns of Table I. As can be seen in Table 1, the trimethylammonium cation head group has characteristic bands at 3016 cm^{-1} (IR, R), 950 cm^{-1}(IR, R), 1441 cm^{-1} (R), and 757 cm^{-1} (R), while the alkyl tail has characteristic bands at 2922 cm^{-1} (IR), 2851 cm^{-1} (IR, R) and 1470 cm^{-1} (IR). These bands may be used as a signature of head or tail respectively.

Vibrational Spectra of Pt-C_{14}TAB

As seen in Figure 2B, the FTIR-DRIFT spectrum of Pt-C_{14}TAB differs from pure C_{14}TAB. The C_{14}TAB spectrum has a 'normal' shape of infrared bands with a full width at half maximum (FWHM) of about 8 – 10 cm^{-1} and C-H stretching bands that have a higher intensity compared to other bands. By contrast, for Pt-C_{14}TAB there appear very broad (FWHM about 300 cm^{-1}), intense bands centered at 1450 cm^{-1} and 760 cm^{-1}, whereas C-H stretching bands are slightly shifted as a result of conformational difference in alkyl chain of pure C_{14}TAB and Pt-C_{14}TAB. Among other factors, it was concluded from SERS study, that not only trimethylammonium head-group, but the hydrophobic alkyl chain are adsorbed flat on the surface of metal as well [7] and the stretching band of CTAB near 2922 cm^{-1} is sensitive to the packing density of the surfactant [3]. As can see in Figure 2B spectrum of Pt-C_{14}TAB along with new broad bands in region below 1500 cm^{-1} has pronounced narrow absorption peaks near 1470 cm^{-1} and 960 cm^{-1}, which are characteristic of free C_{14}TAB. The presence of some amount of nonbonded C_{14}TAB in Pt-C_{14}TAB sample is result of surfactant double layer (tail-to-tail) formation during the synthesis of Pt nanoparticles in aqueous solution and external layer of free C_{14}TAB was difficult remove completely [4]. The UV-Raman spectrum of Pt-C_{14}TAB displayed a very weak intensity with no sign of resonance or SERS enhancement, unlike the case for the PVP/Pt spectrum [5]. This lack of enhancement is most likely due to the inability of the trimethylammonium head group to form a charge-transfer bond with the surface platinum and to the weak absorbance of light in the region of the laser excitation wavelength at 244 nm (Figure 3)

Thermal decomposition of C_{14}TAB and Pt-C_{14}TAB

C_{14}TAB thermal decomposition in N_2, H_2 and O_2. It was shown formerly that the thermal decomposition of quaternary methylammonium halides in Ar atmosphere leads to equimolecular mixtures of two gaseous products: $[N^{+}(CH_3)_4]Br^{-} \rightarrow N(CH_3)_3^{(g)} + CH_3Br^{(g)}$. The kinetics of thermal decomposition is a first-order process with a unimolecular mechanism [10]. The mechanism of thermal decomposition of C_{14}TAB and tetramethylammonium bromide should be similar in appearance, since both cations, $[-CH_2-N^{+}(CH_3)_3]Br^{-}$ and $[H_3C-N^{+}(CH_3)_3]Br^{-}$, have a tetrahedral geometry and similar electronic structure. We present data as 3D graphs, since in this way we can see both the transformation of C_{14}TAB and the appearance of intermediates. As can be seen in the 3D representation of the FTIR-DRIFT spectra of C_{14}TAB vs. temperature (Figure 4, A-C), the thermal decay of C_{14}TAB in N_2 and H_2/Ar atmosphere is accompanied by a pronounced decrease in the intensity of the bands in region 853-964 cm^{-1} which is assigned to $N^{+}C_4$ vibrations of cationic head (Table 1). These bands disappeared above 200 °C simultaneously with the band at 3016 cm^{-1}, which is attributed to the characteristic C-H stretching vibration of the trimethylammonium cation [8]. However, the characteristic bands of the alkyl tail remain until a higher temperature of about 330°C is reached. This data evidenced that: i) N_2 and H_2 atmosphere had no noticeable impact on the thermal unimolecular decomposition of C_{14}TAB; ii) the reaction equation may be presented as $[H_{29}C_{14}N^{+}(CH_3)_3]Br^{-} \rightarrow BrC_{14}CH_3^{(s)} + N(CH_3)_3^{(g)}$, in which trimethylamine escapes into the gas phase but tetradecylbromide remains on the surface until the temperature reaches 300 °C, which is close to its boiling point of 326 °C; iii) in the oxygen atmosphere, the release of trimethylamine into the gas phase is accompanied by oxidation of the alkyl tail to aldehydes (appearance new bands at 2816, 2670, 1717 cm^{-1})

and further aldol condensation to products, which adsorbed on the Al support up to 350 °C .

Pt-CTAB decay in N_2, H_2 andO_2.

The thermal decomposition of capping agent in Pt-C_{14}TAB is substantially different from the decomposition of pure C_{14}TAB. Figure 4 (A*, B*, C*) shows that while the intensity of CH_2 stretching bands at 2922 and 2851 cm^{-1} decrease with increasing temperature, the intensity of the broad bands centered at 1450 and 760 cm^{-1} increase. The primary contribution of the integral intensity in the region of 3020-2800 cm^{-1} is attributed to CH_2 stretching modes of the hydrocarbon tail, and the contribution in 900-500 cm^{-1} region is attributed primarily to the N^+C_4 modes of the ammonium cation head. These integral intensity values can be used for the evaluation of the relative concentrations of hydrocarbon tail and ammonium cation head during heating for both the pure C_{14}TAB and for Pt-C_{14}TAB. As can be seen in Figure 5a in the case of thermal decomposition of pure C_{14}TAB, characteristic band intensities for both the tail and the head decrease since surfactant molecular decomposition produces equimolecular mixtures of trimethylamine and tetradecylbromide. However, in the case of Pt-C_{14}TAB, these band intensities change in the opposite direction. The intensity of the broad band attributed to head of the capping surfactant centered at 760 cm^{-1} increases along with increasing temperature while the intensity of CH_2 stretching vibrations of the tail decrease, a tendency seen in N_2, H_2/Ar, and O_2 atmospheres. The presence of free C_{14}TAB (bands at 1470 cm^{-1} and 960 cm^{-1}) and adsorbed water in the samples of Pt-C_{14}TAB complicate 3D picture in the temperature range 30 °C - 150 °C. It is believed that the FTIR and TGA data (Figure 5b) obtained for thermal decomposition of C_{14}TAB adsorbed on Pt nanoparticles indicates

that above 200°C, the platinum surface becomes coated with a dense layer of ammonium cations without hydrocarbon tails (Figure 5c). The mechanism of thermal degradation of C_{14}TAB adsorbed on Pt nanoparticles is differ in N_2, 10% H_2/Ar, and O_2 environments but in all instances the final residue on the surface of Pt nanoparticles was ammonium derivative. Platinum nanoparticles show the ability of a trap for ammonium moiety. In this paper we do not analyze chemical transformation of C_{14}TAB on Pt surface with full details, e.g. appearance in hydrogen atmosphere N-H bands at 3080 cm^{-1}, 2950 cm^{-1} and at 2764 cm^{-1} characteristic of primary and secondary amine respectively (Figure 6), since 3D graphs revealed clear, that head-group remain on the platinum surface up to 350 °C but analysis of 2D-spectra in detail will be separate subject. The coating of ammonium cations on the Pt surface was found to be thermo-stable up to 350° C. To test the effect of the ammonium layer on accessibility of platinum, we studied the chemisorption of carbon monoxide on Pt-C_{14}TAB after reducing the nanoparticles in 10% H_2/Ar flow at different temperatures.

Carbon monoxide as a probe of accessible Pt surface.

Carbon monoxide is widely used as a probe of the surface accessibility of Pt nanoparticles, since the adsorbed amount of CO is easily controlled [11]. The value of FTIR spectroscopic measurements of band intensity for chemisorbed CO reflects the accessible platinum surface, whereas the position of the CO band reflects both the structure of the surface species and the electronic state of Pt. We studied the FTIR spectra of CO chemisorbed on Pt-C_{14}TAB nanoparticles subjected to reduction in hydrogen at temperatures ranging from 50-200°C. Pt-C_{14}TAB nanoparticles were drop-casted on aluminum foil and then exposed to 10% H_2/Ar flow at 50° C for 10 minutes in a DRIFTS

cell. Afterwards, the system was pumped down to ~10^{-5} torr and then re-pressurized with 350 torr of CO. The sample was then cooled to room temperature (30° C) and spectra were recorded. Finally, the system was pumped down to ~10^{-2} torr at room temperature and spectra were again recorded. This procedure was repeated with the same sample for 10% H_2/Ar treatments at 50 °C, 100 °C, 150 °C, and 200 °C with CO pressures ranging from 300 – 350 torr. Figure 7 illustrates that after treatment of Pt-C_{14}TAB nanoparticles in H_2/Ar and exposure to CO, the rotational-vibrational fine structure of CO in the gas phase appeared along with three new bands at 2040, 1864 and 1780 cm^{-1} in the IR spectrum, which may be attributed to linear (2040 cm^{-1}) and bridging structures of surface carbonyls (Figure 7a). Pumping down the sample to 10^{-4} torr did not change the band intensities of these adsorbed species (Figure 7b). The effect of reduction temperature on the carbonyl bands is shown in Figure 8a and 8b. Two evident conclusions may be drawn: i) Intensities of carbonyl bands after sample treatment in H_2/Ar up to 200°C decreased, and above 200°C, all carbonyl bands can no longer be observed, which suggests that the ammonium cation layer shields the platinum surface completely; ii) the position of CO band maxima as well as the shape and full width at half maximum did not depend on the temperature of reduction. This implies that the oxidation state of Pt atoms on the surface did not change during reduction at temperatures up to 200 °C. The C_{14}TAB cationic capping agent decreases the capability of surface Pt atoms to contribute in $d\pi \rightarrow \pi^*$ back bonding, resulting in an increased frequency of the CO stretch vibration to 2040 cm^{-1} .The value of binding energy for Pt $4f_{7/2}$ line at 74.8 eV indicates, that the formal oxidation state of surface Pt is close to Pt(IV) [12]. In the C_{14}TAB/Pt→CO, the CO bands at 2040 cm^{-1} are asymmetric with a long tail on the low

frequency side. The development of an asymmetric band shape of CO may be due to the inhomogeneities of the platinum surface or result of an 'electron-hole damping' [12]. The FTIR study of nanoparticles with narrow size distribution (Figure 1A) minimized the effect of support inhomogeneity, therefore asymmetry for stretch modes of CO may be produced by an 'electron-hole damping' mechanism [12].

The origin of broad bands at 1450 cm^{-1} and 760 cm^{-1}

The IR spectra shown in Figure 2B indicate that the spectrum of Pt-C_{14}TAB (initial sample at 35 °C) has several narrow characteristic bands of pure C_{14}TAB ((bands at 1470 cm^{-1} and 960 cm^{-1}), since the solution of Pt-C_{14}TAB deposited on Al foil contains some quantity of free C_{14}TAB molecules, which are not bonded to the Pt surface. This is evident also from TGA measurements for both Pt-C_{14}TAB (Figure 5b) and Au-CTAB [4]. Free surfactant decay starts above 200 °C in N_2 and H_2 flow, and at elevated temperatures, we can resolve only the spectra of C_{14}TAB bonded to the platinum surface (Figure 4). The intensity of C-H stretching vibrations at 2917 cm^{-1} and 2850 cm^{-1} ($I_{\Sigma CH}$) may be used as an internal reference for the evaluation of band intensities centered at 1450 and 760 cm^{-1}, since it is believed that the integral intensities of stretching modes of the hydrocarbon tail $-(CH_2)_{14}CH_3$ is relatively constant. The ratio of integral intensities $I_{1450}/I_{\Sigma CH}$ and $I_{760}/I_{\Sigma CH}$ in case of Pt-C_{14}TAB are near 10^2 times higher than in case of pure C_{14}TAB (Figure 9b, 9c). The nature of the broad and intense bands at 1450 cm^{-1} and 760 cm^{-1} is unclear. We have considered two possibilities for the origin of these abnormal bands: i) effect of Surface-enhanced infrared absorption (SEIRA) and ii) the effect of electron-molecular vibration coupling, or in other words the interaction of platinum conducting electrons with intramolecular vibrations of adsorbed C_{14}TAB. The

mechanism of the SEIRA origin is identical to that of SERS. The strong enhancement was observed on the surfaces of coinage metals: Cu, Ag and Au [14], but platinum nanoparticles display very weak surface electromagnetic enhancement. Characteristics of SEIRA show equal enhancement of all IR bands and reveal no broadening [14], contrary to what we have observed. Thus, the origin of the broad bands at 1450 cm^{-1} and 760 cm^{-1} is not related to the SEIRA effect.

There is reason to believe that the abnormally intense bands observed in the Pt-C_{14}TAB spectrum are due to the interaction of conducting electrons of platinum nanocrystals with the intramolecular vibrations of the adsorbed trimethylammonium cations. The manifestation in the IR spectrum of Pt-C_{14}TAB resembles the IR spectra of conducting organic compounds. Formerly, it was shown that in linear chain electron-conducting organic ion-radical salts , a normal infrared spectrum with many narrow bands transformed into a spectrum with only a few broad, high intensity bands, e. g. in triethylammonium tetracyanoquinodimethane ($TEA(TCNQ)_2$) [15]. In a similar manner, IR spectra of 2D organic conductors turn into wide, intense spectra [16]. Rice developed a theoretical model, that explain the remarkable rise of absorption and broadening of IR bands in organic compounds like $TEA(TCNQ)_2$ [17]. The new IR bands are resulting from the electron-molecular vibration coupling (*e - mv* coupling) of the conduction electrons to the symmetric vibrations of the molecule. Hamiltonian for cation-radical molecule may be express as $H = H_e + H_v + \sum g_\alpha n_i Q_{\alpha,i}$ where H_e and H_v describe, respectively, the radical electrons and the symmetric intramolecular vibrations in the absence of vibronic coupling. The term $\sum g_\alpha n_i Q_{\alpha,I}$ - express *(e-mv)* coupling, where $Q_{\alpha,i}$ denotes the normal-mode coordinate corresponding to the symmetric vibration and g_α

are *(e-mv)* constants, which differ from zero only for symmetrical vibrations [17, 18]. Initially 'normal' intramolecular symmetrical vibrational modes, which are Raman active, transform into high intensity electron-vibrational modes. All previously studied systems were ionic or ion-radical organic salts with high electron conductivity [19]. The proof of *e-mv* coupling in quasi-one dimensional crystals is the fact that new IR bands are polarized in the direction of the maximal conductivity axis in anisotropic crystals [14, 15, and 18]. In the case of Pt-C_{14}TAB nanoparticles, the layer of organic cations (TMA) on the surface of platinum nanoparticles is oriented randomly relative to the polarized IR beam, and an experiment with polarized light did not show noticeable differences for s- and p-polarization. Application of *(e - mv)* coupling mechanism to the Pt-C_{14}TAB interface results in an electron transition which may occur from Pt nanoparticles to adsorbed ammonium cations under IR irradiation, forming a short-lived cation-radical $RN^{+}(CH3)3 + e^{-} \rightarrow RN^{*+}(CH3)3$. In accordance with Rice's mechanism, relaxation of the ammonium cation-radical will be accompanied by excitation of symmetrical vibrational modes of the trimethylammonim cation, which are active in Raman spectrum but inactive in the IR spectrum [17, 15]. The Raman spectrum of C_{14}TAB has intense bands at 1441 cm^{-1} and 757 cm^{-1} that are attributed to non-degenerate symmetrical A_1 vibrations of type $\delta(N^{+}(CH_3)_3)$ and $\nu(N^{+}C_4)$ of the trimethylammonium cation respectively (Figure 9a, Table 1). The position of these Raman bands for C_{14}TAB coincides with the new broad infrared absorption bands centered near 1450 cm^{-1} and 760 cm^{-1}, in accordance with the prediction from the Rice's theoretical model [17] for *(e - mv)* coupling. Thus, the data obtained may be considered as an indication of a strong

interaction between conducting electrons of Pt nanoparticles and molecular vibrations of adsorbed trimethylammonium cations.

CONCLUSIONS

We have shown that the thermal decay of Pt-C_{14}TAB nanoparticles in N_2, H_2/Ar, and O_2 atmospheres leads to the release of the hydrocarbon 'tail' and the formation of a strongly bonded layer of ammonium cations on the platinum surface. Above 200 °C, the surface of Pt nanoparticles become inaccessible to the chemisorption of carbon monoxide since it is shielded by trimethylammonium cations. The oxidation state of the platinum surface that was accessible to CO chemisorption was not reduced by hydrogen in the temperatures ranging from 30-200 °C. The adsorbed layer of ammonium cations 'conserve' the electronic state of surface platinum atoms. We propose that the origin of unusually high-intensity broad bands centered at 1450 cm^{-1} and 760 cm^{-1} results from the interaction between conducting electrons of Pt nanoparticles and molecular vibrational modes of A_1 type of adsorbed ammonium cations. This electron-molecular vibration coupling transforms the initially 'normal' intramolecular vibrational modes into high intensity electron-vibrational modes.

ACKNOWLEDGMENT

This work was supported by the Director, Office of Science, Office of Basic Energy Sciences, Division of Chemical Sciences, Geological and Biosciences of the U.S. Department of Energy under Contract No. DE-AC02-05CH11231

REFERENCES

1 Lee, H.; Habas, S. E.; Kweskin, S. J.; Butcher, D.; Somorjai, G. A.; Yang, P. *Angew. Chem. Int. Ed.* **2006**, 45, 7824.

2 Sui, Z.M.; Chen, X.; Wang, L.Y.; Xu, L.M.; Zhuang, W.C.; Chai, Y.C.; Yang, C.J. *Physica E,* **2006**, 33, 308.

3 Li, H.; Tripp, C.P. *J. Phys. Chem. B* **2004**, 108, 18318. *Langmuir* **2002**, 18, 9441 (a). Kung, K.-H.S.;Hayes, K.F. *Langmuir* **1993**, 9, 263. Ninness, B.J.; Bousfield, D.W.; Tripp, C.P. *Colloids Surf., A* **2002**, 203, 21

4 Nikoobakht, B. and El-Saed, M.A. *Langmuir* **2001**, 17, 6368.

5 Authors are indebted to Dr. Jeong Park who provides us with XPS data.

6 Borodko, Y.; Habas, S.E.; Koebel, M.; Yang, P.; Frei, H. and Somorjai, G.A. *J. Phys. Chem. B* **2006**, 110, 23052. Borodko, Y.; Humphrey, S.M.; Tilley, T.D.; Frei, H. and Somorjai, G.A. *J. Phys. Chem. C* **2007**, 111, 6288.

7 Koglin, E.; Tarazona, A.; Kreisig, S.; Schwuger, M.J. *Colloids Surf. A*, **1997**, 123-124, 523

8 Ebsworth, E.A.V. and Sheppard, N. *Spectrochimica Acta*, **1959**, 13, 261.

9 Colthup, N.B. and Daly, L.H. *Introduction to Infrared and Raman Spectroscopy*, Acad. Press, San Diego, **1990**

10 Sawicka, M.; Storoniak, P.; Skurski, P.; Blazejowski, J; Rak, J. *Chem. Phys.* **2006**, 324, 425.

11 Little, L.H. *Infrared Spectra of Adsorbed Species*, Acad. Press, London, New York, **1966**

12 Moulder, J.F.; Stickle,W.F.; Sobol, P.E. and Bomben, K.D. in Chastain, J. (Ed), Handbook of X-ray Photoelectron Spectroscopy, Perkin-Elmer Corp., 1992

13 Langreth, D.C. *Phys. Rev. Letters,* **1985**, 54/2, 126. Crljen, Z.; Langreth, D.C. *Phys. Rev. B,* **1987**, 35/9, 4224. Fano, U. *Phys.Rev.* **1961**, 124/6, 1866.

14 Aroca, R. *Surface-Enchanced Vibrational Spectroscopy*, J. Wiley, Chichester, England **2006**. Aroca, R., Price, B. J. *Phys. Chem. B* **1997**, 101, 6537.

15 Kaplunov, M.G.; Panova, T.P. and Borodko, Y.G. *Phys. Status Solidi (a)* **1972**, 13, K67. Brau, A.; Bruesch, P.; Farges, J.-P.; Hinz, W. and Kuse, D. *Phys. Status Solidi (b)* **1974**, 62, 615. Graja, A. *Low-Dimensional Organic Conductors. World Sci., Singapore,* **1992**.

16 Sugano, T.; Yamada, K.; Saito, G. Kinishita, M. *Solid State Comm.* **1985**, 55/2, 137. Jacobsen, C.S.; Williams, J.M.; Wang, H.H. *Solid State Comm.* **1985**, 54/11, 937.

17 Rice, M.J. *Phys. Rev. Lett.* **1976**, 37/1, 36. Rice, M.J.; Pietronero, L.; Bruesch, P. *Solid State Comm.* **1977**, 21, 757. Rice, M.J. *Solid State Comm.* **1979**, 31, 93

18 Kaplunov, M.G.; Borodko, Y.G. *Chem. Phys.(Russian),* **1987**, 6/11, 1529. Kaplunov, M.G. *Solid State Physics (Russian),* **1978**, 20/5, 1529.

19 *Organic Conductors: Fundamentals and Applications.* Ed. Farges, J.-P., Marcel Dekker, New York, **1994**.

FIGURE CAPTIONS

Figure 1. A) TEM image of C_{14}TAB stabilized Pt nanoparticles (12 ± 2 nm);
B) SEM image of a Langmuir-Blodgett film of Pt-C_{14}TAB deposited on a Si wafer.

Figure 2. a) FTIR-DRIFT and UV-Raman spectra of pure C_{14}TAB deposited on Al foil as a cast film. b) Comparison of FTIR-DRIFT spectra of pure C_{14}TAB and Pt-C_{14}TAB.

Figure 3. Diffuse reflectance spectra in the UV-region of a thick layer of pure C_{14}TAB and a thin layer of Pt-C_{14}TAB, which was magnified to normalize both spectra (both samples were deposited on Al foil).

Figure 4. FTIR-DRIFT spectra of pure C_{14}TAB heated in flow of N_2 (2.5 °C/min) (A), in flow of H_2/Ar (B) and in flow of O_2 (C) and spectra of Pt-C_{14}TAB heated in flow of N_2 (A*), H_2/Ar (B*), and in O_2 (C*).

Figure 5. a) The change in intensities for characteristic bands of tail (stretch CH_2) and head (stretch N^+C_4) during heating (3.2 °C/min) for pure C_{14}TAB in H_2 (▲-tail, △-head, dotted lines) and Pt-C_{14}TAB in H_2 (■ -tail, □-head, solid lines). b) TGA plots (10 °C, N_2) for C_{14}TAB (A, C) and Pt-C_{14}TAB (B, C). A sharp weight loss near 100 °C reflects the loss of water and above 200 °C, the loss of hydrocarbon tails. c) Schematic illustration of the complete coating of Pt nanoparticles by cationic heads (tail-off) at temperatures above 200 °C.

Figure 6. FTIR spectra of Pt-C_{14}TAB heated in flow of H_2/Ar (10%H_2) above 200 °C show appearance new bands at 3080 cm^{-1}, 2950 cm^{-1} and 2764 cm^{-1}, which may

be assigned to to stretching modes of $^{+}NH_2$ and ^{+}NH groups [8]. The spectra at high temperature were increased by multiplication.

Figure 7. FTIR spectra of Pt-C_{14}TAB with gas phase CO (a), after pump-out of gaseous CO (b), and initial Pt-C_{14}TAB in the range of 1700-2300 cm^{-1} (c).

Figure 8. FTIR-DRIFT spectra of carbon monoxide adsorbed on Pt-C_{14}TAB: a) Reduced in hydrogen at different temperatures; b) The effect of heating Pt-C_{14}TAB nanoparticles in H_2 on integral intensities of carbonyl bands

.Figure 9. A) A comparison of a Raman spectrum of pure C_{14}TAB (a) and FTIR-DRIFT spectra of pure C_{14}TAB (b) and Pt-C_{14}TAB (c). The position of intense broad bands at 1450 and 760 cm^{-1} is close to the position of nondegenerate A_1 type stretches of the trimethylammonium cation at 1441 and 757 cm^{-1}.

B) The thermal degradation of Pt-C_{14}TAB monitored by *in-situ* FTIR-DRIFT spectra measurements. For comparison, the spectrum of pure CTAB is shown. As can be seen, ammonium cations are firmly bonded to platinum up to 340 °C.

TABLE 1
IR and UV-Raman Bands (cm^{-1}) Assignments for $C_{14}TAB$ and Pt-$C_{14}TAB$

IR $C_{14}TAB$	IR Pt-$C_{14}TAB$	Raman $C_{14}TAB$	Raman Pt-$C_{14}TAB$	assignments [7-9]
3016	3015	3016		CH_{3asym} ($-N^+(CH_3)_3$)
2946_{sh}		2943		CH_{3sym} ($-N^+(CH_3)_3$)
2922	2917			CH_{2asym}
	2887	2883		
2851	2849	2850		CH_{2sym}
			1618	H_2O_{def}
	1575			
1485				$\delta(CH_3)_{asym}$
1471	1470_{broad}			$(CH_2)_{def}$
1464		1462		$(CH_2)n_{sciss}$
		1441	1441	$\delta(N^+CH_3)_{sym}$, A_1
1406				
1395		1398	1396	
	1372			
	1331	1295	1288	
		1125	1167	
		1061		
964		957		CN^+
950				
913		910		
	853			
			834	R_{Td} $-H_2C-N^+(CH_3)_3$
802				
		757		$C_4N^+_{sym}$ A_1
730				
720				CH_{2rock}
	634vs			
			546	
500				$\delta(C_4N^+)$
		448	426	
			340	

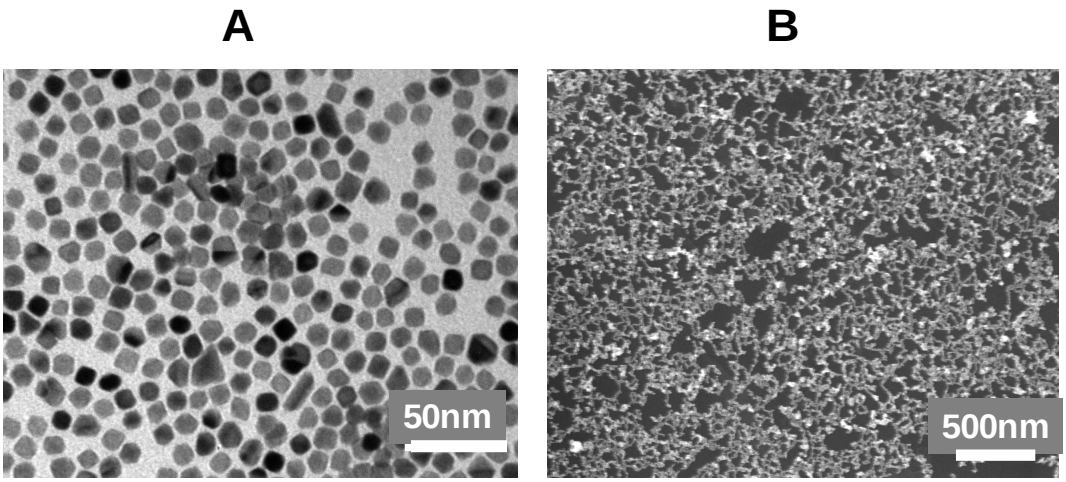

Figure 1

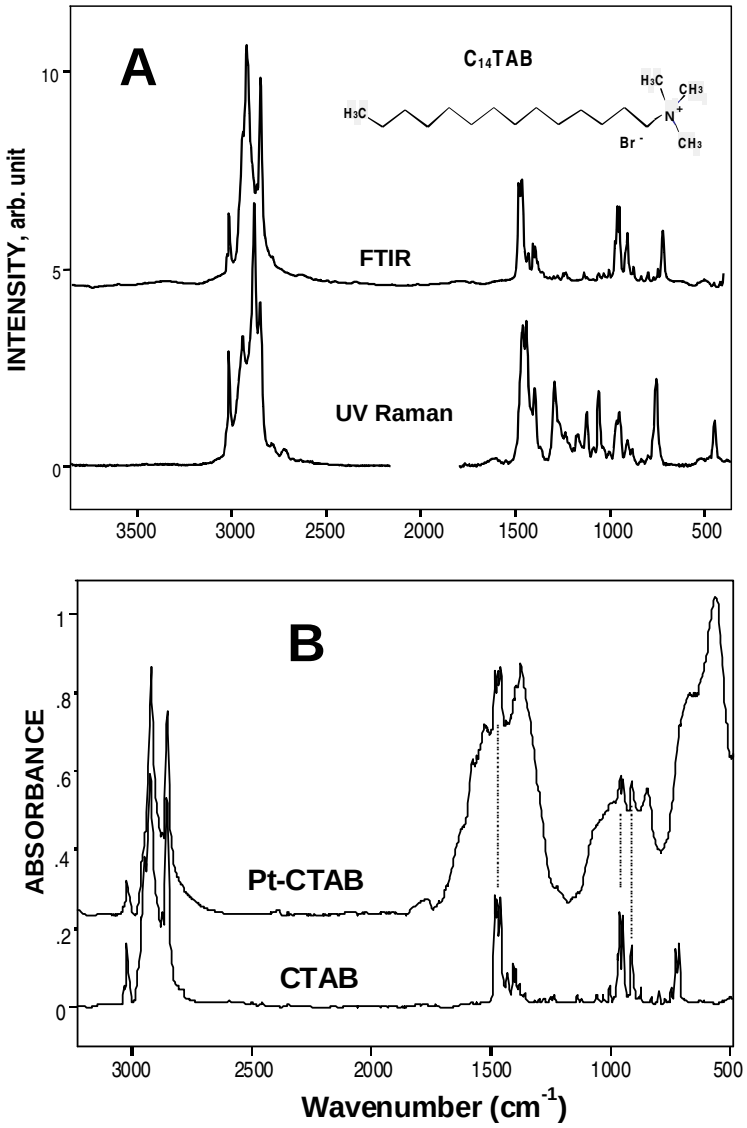
A
C14TAB
H3C
CH3
H3C
N+
Br -
CH3
INTENSITY, arb. unit
10
5
0
FTIR
UV Raman
3500
3000
2500
2000
1500
1000
500
B
ABSORBANCE
1
.8
.6
.4
.2
0
Pt-CTAB
CTAB
3000
2500
2000
1500
1000
500
Wavenumber (cm-1)

Figure 2

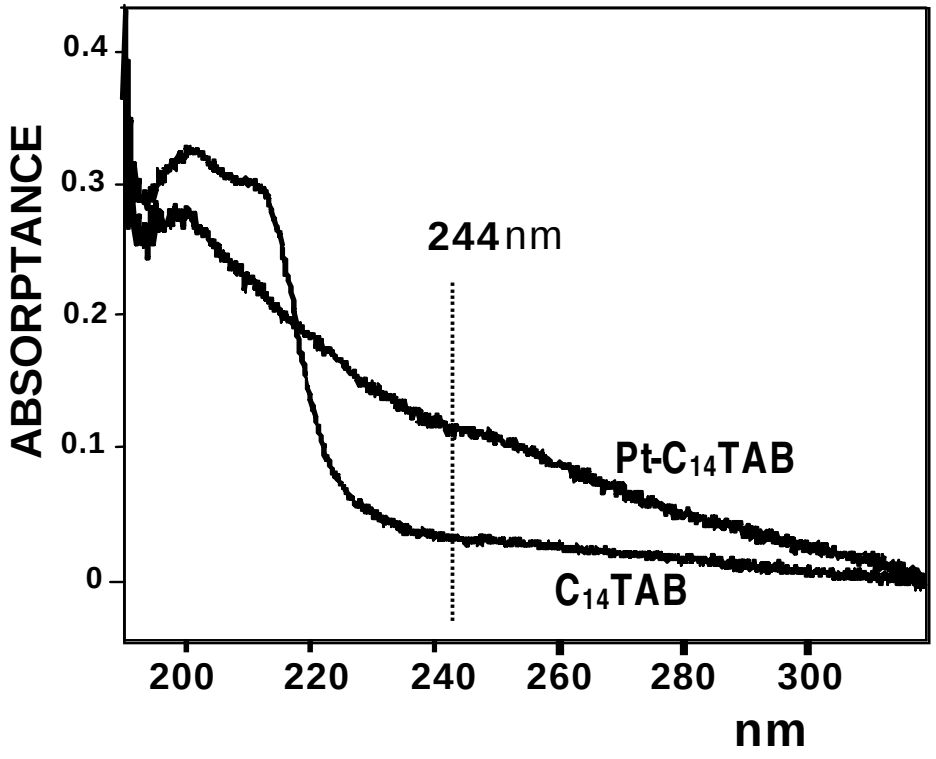
ABSORPTANCE
0.4
0.3
0.2
0.1
0
244nm
Pt-C14TAB
C14TAB
200
220
240
260
280
300
nm

Figure 3

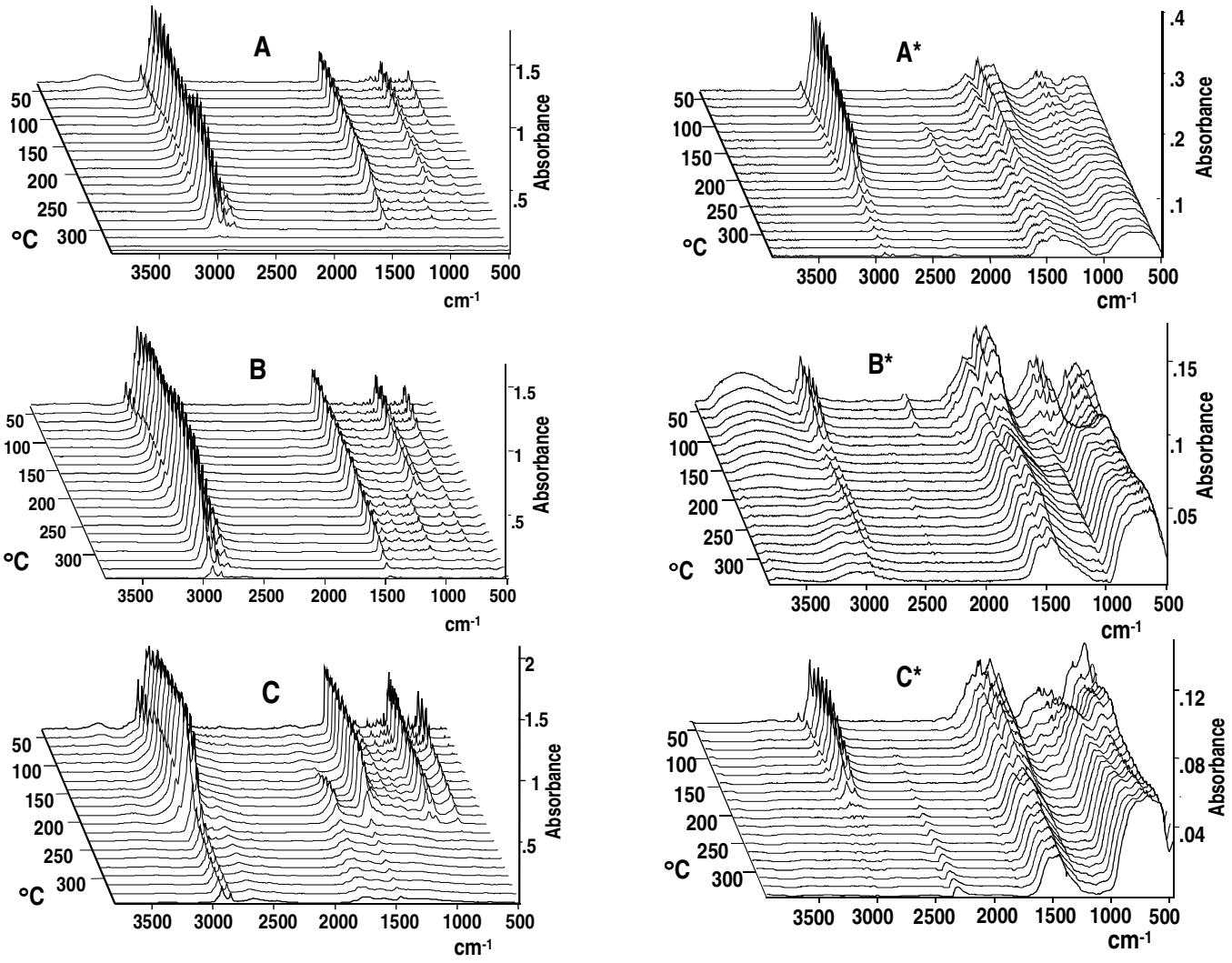
A
A*
B
B*
C
C*
°C
50
100
150
200
250
300
3500
3000
2500
2000
1500
1000
500
cm-1
Absorbance

Figure 4

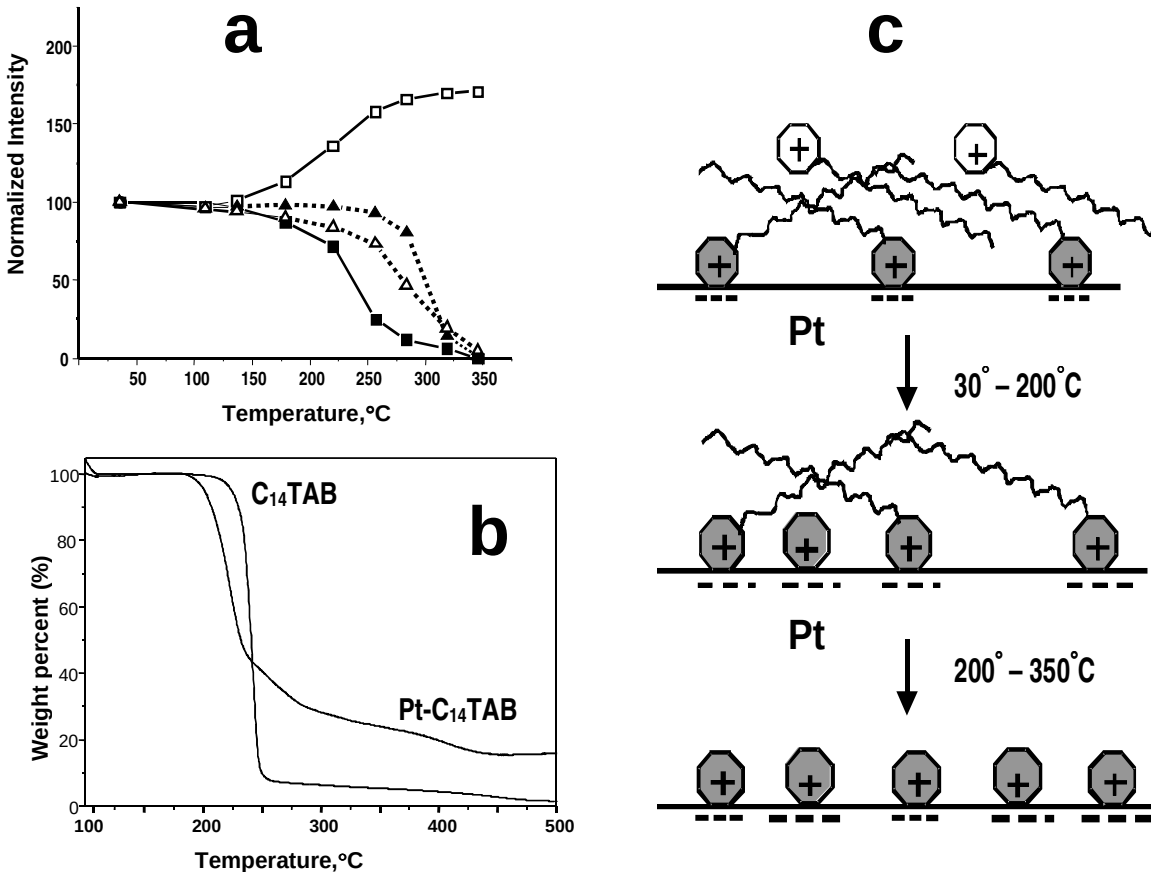
a
Normalized Intensity
Temperature,°C
b
C14TAB
Pt-C14TAB
Weight percent (%)
Temperature,°C
c
Pt
30° – 200°C
Pt
200° – 350°C

Figure 5

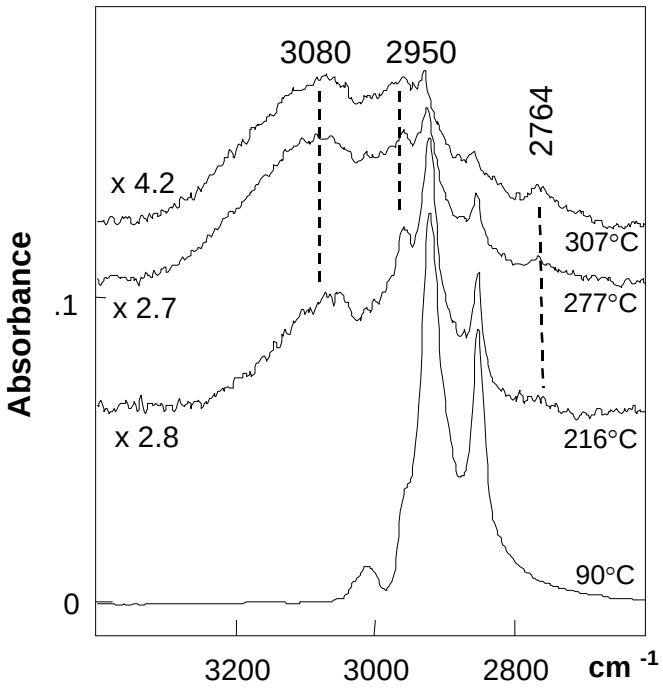
3080
2950
2764
x 4.2
307°C
x 2.7
277°C
x 2.8
216°C
90°C
Absorbance
.1
0
3200
3000
2800
cm -1

Figure 6

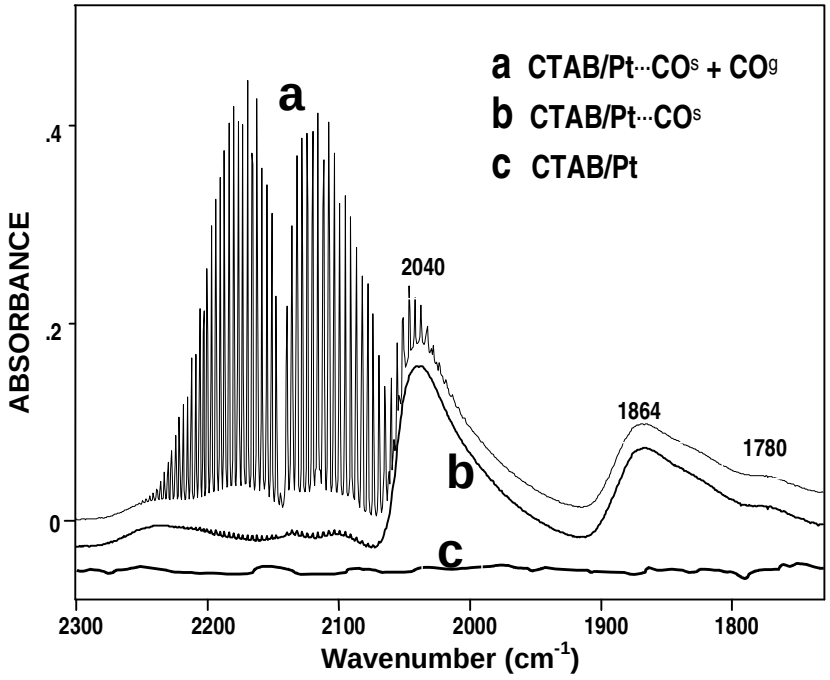
a CTAB/Pt···CO^s + CO^g
b CTAB/Pt···CO^s
c CTAB/Pt
a
b
c
2040
1864
1780
ABSORBANCE
.4
.2
0
2300
2200
2100
2000
1900
1800
Wavenumber (cm-1)

Figure 7

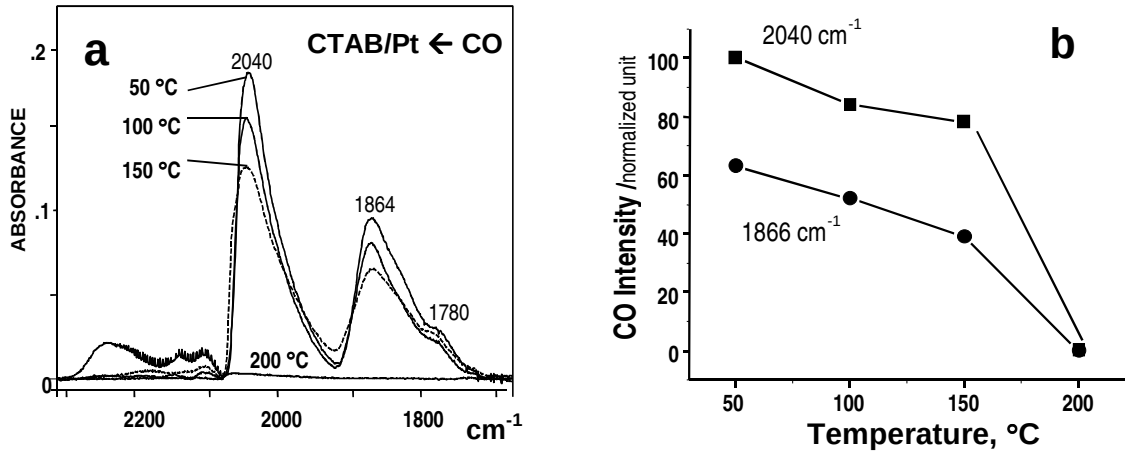
a
CTAB/Pt ← CO
2040
50 °C
100 °C
150 °C
1864
1780
200 °C
ABSORBANCE
.2
.1
0
2200
2000
1800
cm-1
b
2040 cm-1
1866 cm-1
CO Intensity /normalized unit
100
80
60
40
20
0
50
100
150
200
Temperature, °C

Figure 8

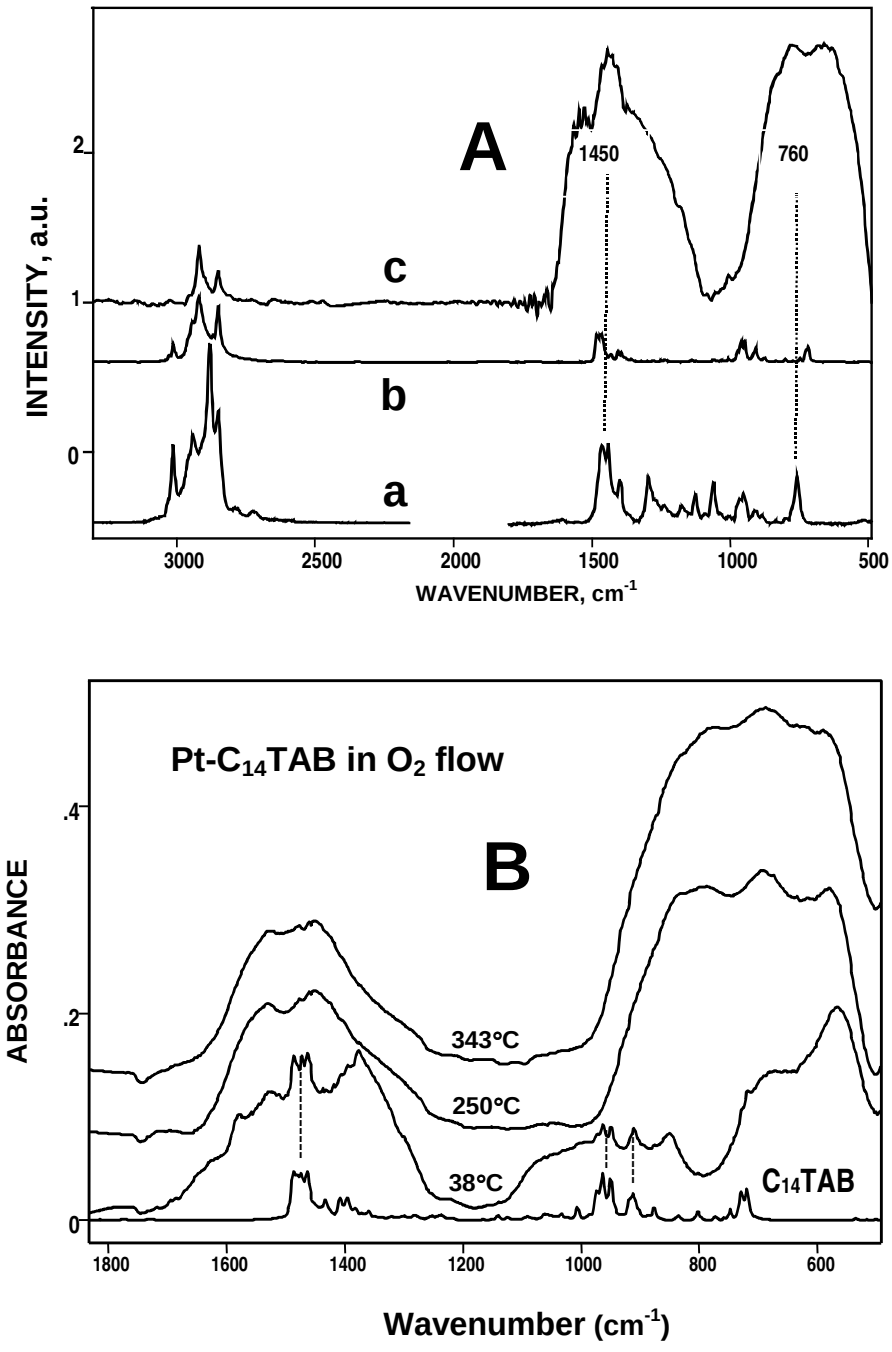
A
1450
760
c
b
a
INTENSITY, a.u.
2
1
0
3000
2500
2000
1500
1000
500
WAVENUMBER, cm-1
Pt-C14TAB in O2 flow
B
343°C
250°C
38°C
C14TAB
ABSORBANCE
.4
.2
0
1800
1600
1400
1200
1000
800
600
Wavenumber (cm-1)

Figure 9